

## Original Article

# Synthesis and evaluation of perfluorooctylbromide nanoparticles modified with a folate receptor for targeting ovarian cancer: in vitro and in vivo experiments

Xinjie Liu<sup>1</sup>, Jiannong Zhao<sup>1</sup>, Dajing Guo<sup>1</sup>, Zhigang Wang<sup>2</sup>, Weixiang Song<sup>1</sup>, Weijuan Chen<sup>1</sup>, Jun Zhou<sup>1</sup>

<sup>1</sup>Department of Radiology, The Second Affiliated Hospital of Chongqing Medical University, No. 74 Linjiang Rd, Yuzhong District, Chongqing 400010, China; <sup>2</sup>Institute of Ultrasound Imaging, Department of Ultrasound, The Second Affiliated Hospital of Chongqing Medical University, No. 74 Linjiang Rd, Yuzhong District, Chongqing 400010, China

Received April 8, 2015; Accepted June 7, 2015; Epub June 15, 2015; Published June 30, 2015

**Abstract:** Background: Epithelial ovarian cancer is the leading cause of death among gynecologic malignancies. However, detecting ovarian cancer at an early stage remains challenging. In this work, we aimed to synthesize a folate-receptor-targeting perfluorooctylbromide nanoparticle (FR-TPNP) as a targeted computed tomography (CT) contrast agent for the early detection of ovarian cancer. Methods: Perfluorooctylbromide (PFOB) was encapsulated in Poly (lactic-co-glycolic acid) (PLGA) by a two-step emulsion technique to construct the nanoparticles. Folate-poly (ethylene glycol)-carboxylic acid (Fol-PEG-COOH) was introduced to modify the surface of the nanoparticles through attachment to the PLGA. The effects of different volume ratios of PFOB to PLGA on the characteristics of the FR-TPNP emulsions were compared. The size distribution and potential of the FR-TPNPs were assessed with a laser particle size analyzer system. The in vitro targeting ability of the FR-TPNPs was observed with a confocal laser scanning microscope (CLSM), and the in vivo transportation of the FR-TPNPs was evaluated with CT. Results: The sizes of the FR-TPNP emulsion with different volume ratios varied from  $302.67 \pm 27.83$  nm to  $563.68 \pm 47.29$  nm, and the mean CT value ranged from  $233 \pm 20.59$  HU to  $587.66 \pm 159.51$  HU. Both the size and mean CT value increased with the volume ratio. The FR-TPNPs showed greater cell affinity and targeting efficiency to SKOV3 cells than the control group and folic acid interference group in vitro, as observed by CLSM. A significant CT enhancement of ovarian cancer xenografts in the targeted group of a nude mice model was observed 2 h post-injection; it increased to a peak at 12 h and had a duration of 48 h. The mean CT value of the tumor in the targeted group was considerably higher than those in the non-targeted and other groups 6 h post-injection. Conclusion: The synthesized FR-TPNP emulsion was an effective CT contrast agent with highly efficient targeting ability and a long circulation time, thus representing a potential strategy for the earlier detection of ovarian cancer.

**Keywords:** Folate receptor, PFOB, ovarian cancer, targeting CT contrast agent

## Introduction

Epithelial ovarian cancer is the leading cause of morbidity and mortality among gynecologic malignancies [1], and the high-grade serous ovarian cancer histotype represents the largest proportion (65%) of cases [2]. CT is widely used to detect primary ovarian cancer and its metastases in clinical settings. However, routine CT can only provide limited information about the tumor itself, such as the number of tumors,

size, shape, and blood supply, and can detect only certain metastases. It is difficult to detect early-stage ovarian cancer using routine CT. Thus, nearly 90% of patients are first diagnosed at stage III/IV, and the five-year survival rate is less than 30% [3]. It is essential to diagnose the disease at an early stage to alleviate the suffering of patients and improve their quality of life.

Recently, the emergence of nanotechnology has improved our ability to detect diseases,

## FR-TPNP as a targeted for early detection of ovarian cancer

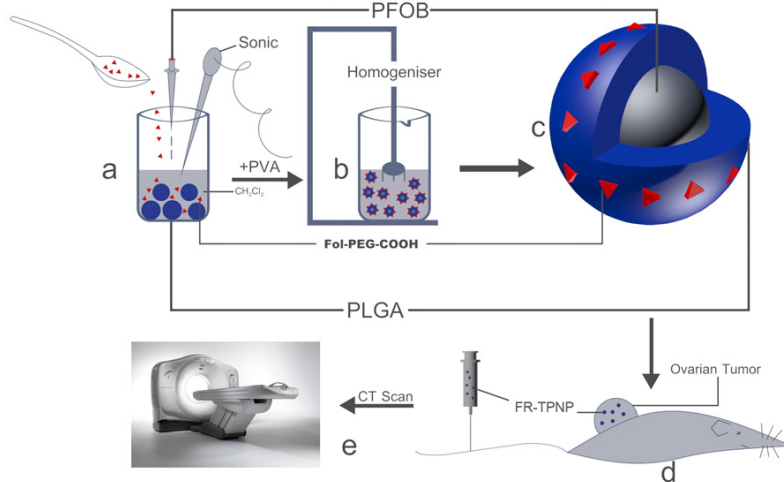


**Figure 1.** Schematic of the formulation process for FR-TPNPs and CT scan.

including cancer, earlier than previously thought [4]. Folate receptor (FR)- $\alpha$  is overexpressed on the surface of ovarian cancer, especially the epithelial type [5], whereas low or negligible expression of FR- $\alpha$  is observed in normal tissue. This observation allows the use of targeted agents for the early diagnosis of tumors. Indeed, several reports have demonstrated the potential of targeted nanoparticles for detecting primary ovarian cancer and micrometastasis [6-8]. These studies have focused on nanoparticles for single photon emission computed tomography (SPECT) and fluorescence imaging. However, the disadvantages of SPECT and fluorescence imaging, such as low spatial resolution and low tissue penetration, may limit the application of these targeting nanoparticles in clinical settings.

CT is one of the most frequently used non-invasive technologies in modern medicine. Numerous advances have been made to make this technique more powerful with improved signal sensitivity, rapid image acquisition and faster reconstruction. The synergistic development of novel nanoparticles, including gold (Au)-, ytterbium (Yb)-, and bismuth (Bi)-based nanoparticles [9-11], have been used to obtain next-generation CT contrast agents for imaging-specific biological markers [12]. All of these novel nanoparticles have several advantages over conventional CT contrast agents. For example, they have a long blood circulation time, high X-ray attenuation and a high capacity for targeted imaging. Despite these advantag-

es, there are still some disadvantages associated with using these nanoparticles, such as the high cost of Au nanoparticles and the difficult synthetic method of Yb and Bi nanoparticles.

PFOB is an eight-carbon chain with only one bromine substituent; the other substituent is fluorine. PFOB is highly biocompatible, and no adverse responses have been observed in humans at oral doses up to 12 ml/kg [13]. A PFOB emulsion has long been used as a CT contrast agent for persistent enhancement of liver and spleen tumors and of VX<sub>2</sub> tumors in a rabbit model [14]. A recent study reported that PFOB nanoparticles can be used as a multimodal contrast agent for CT, US and MRI molecular imaging [15]. Barnett et al. [16] prepared rhodamine-PFOB nanoparticles for use in the non-invasive multimodal cell tracking of human pancreatic islets. These studies have demonstrated the great potential of PFOB nanoparticles in nanotechnology.

Poly (lactic-co-glycolic acid) (PLGA) is one of the most widely used polymers because of its biocompatibility, and it is degraded to monomers of lactic acid and glycolic acid in the body [17]. PLGA nanoparticles or micelles can be easily prepared with various designs [18]. Furthermore, PLGA can be used to carry multiple ligands for cancer targeting and imaging molecules for cancer diagnostics via simple conjugation-based structural modifications [19].

In this study, we aimed to combine the advantages of PFOB and PLGA with modifications of Fol-PEG-COOH to develop FR-targeted perfluorooctylbromide nanoparticles (FR-TPNPs) and to investigate their related characteristics, targeting ability, and CT contrast-enhancing potential and behavior. The synthetic process of FR-TPNPs and an in vivo CT scan are shown in **Figure 1**. We expected to obtain an efficient CT contrast agent with high biocompatibility and the capability for active targeting to detect early-stage ovarian cancer.

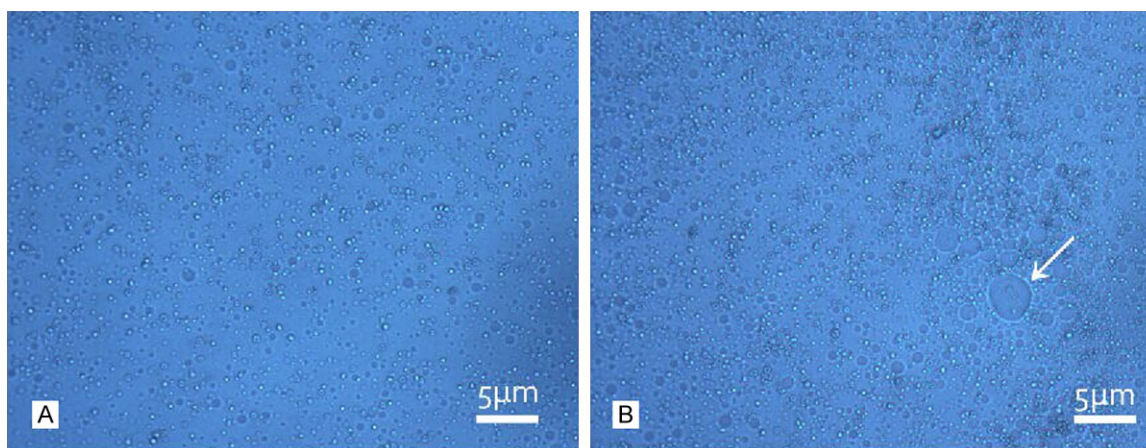


**Figure 2.** Optical microscopy images of the prepared FR-TPNP emulsions ( $\times 400$ ). A. Optical microscopy image of the FR-TPNP emulsion at a volume ratio of 1:2, bright dots indicate the uniform nanoparticles; B. Optical microscopy image of the FR-TPNP emulsion at a volume ratio of 1:1. The nanoparticles were not uniform, and many had oil between them. The arrow indicates an oil-like droplet.

**Table 1.** Characteristics of FR-TPNPs

	Size (nm)	PDI	Zeta potential (mV)
FR-TPNPs (1:1)	563.68 $\pm$ 47.29	1.19 $\pm$ 0.73	-18 $\pm$ 2.43
FR-TPNPs (1:2)	359.38 $\pm$ 33.60	0.38 $\pm$ 0.083	-15 $\pm$ 4.18
FR-TPNPs (1:4)	313.98 $\pm$ 25.46	0.53 $\pm$ 0.047	-18 $\pm$ 3.11
FR-TPNPs (1:8)	302.67 $\pm$ 27.83	0.42 $\pm$ 0.063	-16 $\pm$ 5.73

FR-TPNPs: folate-receptor-targeting perfluorooctylbromide nanoparticle.

## Methods

### Materials

PLGA, at a lactide/glycolide molar ratio of 50:50 and with a molecular weight of 10,000 Dalton (Da), and Fol-PEG-COOH, with a molecular weight of 3,000 Da, were both purchased from B H Bio Science (Shanghai) Co., LTD. (Shanghai, China). PFOB, at a concentration of 98%, and polyvinyl alcohol (PVA) were purchased from Sigma-Aldrich Corporation (Missouri, USA). RPMI 1640 medium and trypsin were purchased from HyClone Laboratories, Inc. (Utah, USA), and fetal bovine serum was purchased from KangYuan Biology Co., Ltd (Tianjin, China). Iohexol was obtained from BeiLu Pharmaceutical Co., Ltd (Beijing, China). All other reagents used were of analytical grade.

### Preparation of the FR-TPNPs

The FR-TPNPs were prepared using a two-step emulsion process. Fol-PEG-COOH (30 mg) and

PLGA (100 mg) were first dissolved in 2 ml of  $\text{CH}_2\text{Cl}_2$ . The mixture was emulsified using an ultrasonic oscillation instrument (VCX130, Sonics & Materials, Inc., CT, USA) at 130 W for 90 s with the dropwise addition of PFOB (the PFOB:PLGA volume ratios were 1:1, 1:2, 1:4, and 1:8). Next, the solution was poured into 10 ml of PVA (3%) and homogenized with a high-speed homogenization dispersion machine (C10, Shanghai HENC Mechanical Equipment Company, Shanghai, China) for 5 min at 20,000 rpm for the second emulsification. Then, 20 ml of 2% isopropanol solution was added, and the mixture was stirred continuously at room temperature for 3-6 h until surface solidification of the nanoparticles and  $\text{CH}_2\text{Cl}_2$  volatilization. The process was performed under ice bath conditions to avoid vaporization of PFOB. Subsequently, the emulsion was centrifuged at 10,000 rpm for 5 min, the supernatant was discarded, and the precipitate was washed with deionized water. The precipitate was collected and stored at 4°C for further use.

The perfluorooctylbromide nanoparticles (PNPs) and pure PLGA nanoparticles were both prepared using the same process without the addition of Fol-PEG-COOH, and the pure PLGA nanoparticles were encapsulated by the addition of water instead of PFOB.

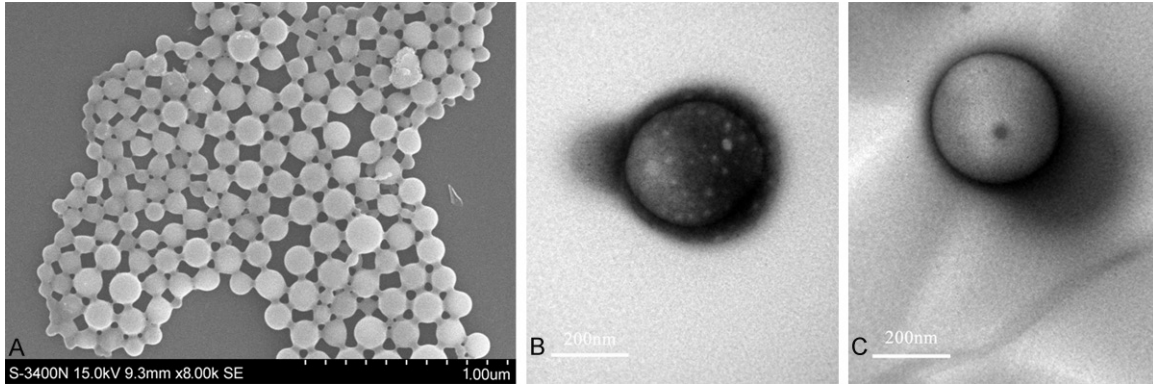


**Figure 3.** SEM and TEM images of FR-TPNPs. A. SEM image of the prepared FR-TPNPs. B. TEM image of the prepared FR-TPNP. C. TEM image of the pure PLGA nanoparticle.

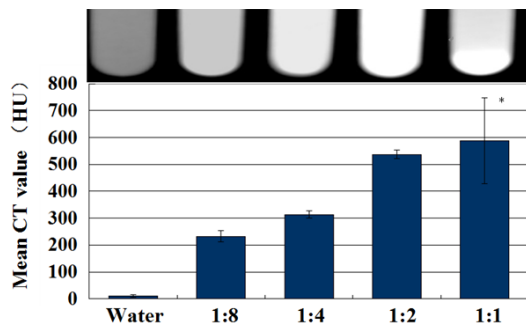


**Figure 4.** In vitro CT images of water and the prepared FR-TPNP emulsions with different ratios. \* $P > 0.05$  compared with the FR-TPNP (1:2) group.

#### Characteristics of the FR-TPNP emulsion

The appearance of the emulsions was observed first, and emulsification with different volume ratios was observed using a light microscope (LM, Olympus, IX71, Japan). A laser particle size analyzer system (Zeta SIZER 3000HS; Malvern, USA) was used to determine the mean sizes and size distribution of the FR-TPNPs. The morphological characterization of the FR-TPNPs was estimated with a scanning electron microscope (SEM, Hitachi, S-3400N; Japan), and the internal structure was observed by transmission electron microscopy (TEM, Hitachi7500, Hitachi Ltd., Tokyo, Japan).

#### In-vitro CT enhanced ability of FR-TPNPs

The CT-enhanced potential of the FR-TPNP emulsion was evaluated using a clinical CT scanner (LightSpeed, GE Healthcare, USA). Water and FR-TPNP emulsions with different volume ratios (1:1, 1:2, 1:4, and 1:8) were placed in an Eppendorf tube 1 cm in diameter.

The scan parameters were as follows: tube voltage, 120 kV; tube current, 200 mA; section thickness, 0.625 mm; pitch, 0.562:1; and field of view (FOV), ped head. The CT values within the region of interest (ROI) of 15 mm<sup>2</sup> were measured three times using a GE ADW 4.3 workstation.

#### In vitro and in vivo target ability of FR-TPNPs

**Cell culture:** The SKOV3 epithelial ovarian cancer cells were obtained from the Ultrasound Engineering Institute of Chongqing Medical University (Chongqing, China). Cells were cultured in PRMI 1640 medium supplemented with 10% heat-inactivated fetal bovine serum in a humidified incubator at 37°C in 5% CO<sub>2</sub>. For the experiments, cells were detached with trypsin and adjusted to the required concentration of viable cells.

**Animal preparation:** All animal experiments were approved by the Animal Ethics Committee of Chongqing Medical University. Twenty BALB/c-nu nude mice (females, 4-6 weeks old, weight of 18-20 g kg) were purchased and fed in the Animal Center of Chongqing Medical University under standard conditions according to the Institute's guidelines. Under sterile conditions, the mice were injected subcutaneously in the right flank with  $5 \times 10^6$  SKOV3 cells suspended in 200  $\mu$ l of PRMI 1640 medium. The tumor-bearing mice were subjected to CT scanning when the subcutaneous tumors reached 0.5-1.0 cm in diameter or 14-21 days after implantation.

**In vitro targeting ability of FR-TPNPs:** Targeting ability was directly observed by CLSM (Leica

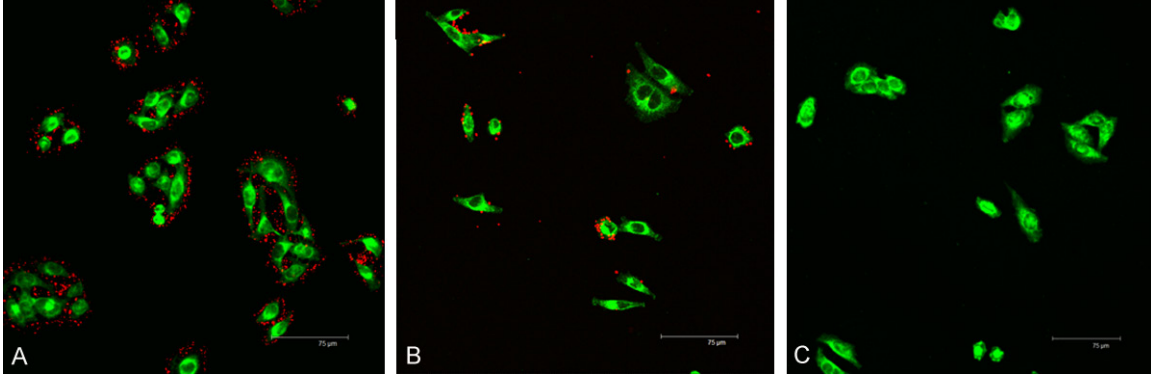


**Figure 5.** In vitro targeting efficacies of the FR-TPNPs (red dots) to SKOV3 cells (green area) observed by CLSM imaging. A. Targeted group; B. Control group; C. Folic acid intervention group.

TCS-SP2, Leica Microsystems, Wetzlar, Germany). SKOV3 cells were seeded in the Confocal Petri dish for 24 h at a density of  $1 \times 10^6$  cells/dish in a humidified incubator at  $37^\circ\text{C}$  in 5%  $\text{CO}_2$ . The cell membrane was stained with Dio, and the FR-TPNPs and PNPs were all stained with Dil before use. Then, the SKOV3 cells were randomized into three groups. FR-TPNPs (200  $\mu\text{l}$ ) were added to the first group, which served as the targeted group. PNPs (200  $\mu\text{l}$ ) were added to the second group, which served as the control group. The last group was given 1 ml of folic acid solution (1 mol/l) 30 min before 200  $\mu\text{l}$  of FR-TPNPs was introduced, which served as the folic acid intervention group. All three groups were incubated for 6 h, and all dishes were then washed repeatedly with PBS to prevent the dissociation of nanoparticles before observation.

*In vivo CT experiment:* Twenty nude mice bearing SKOV3 xenografts were randomized into 4 groups (5 mice in each group). The targeted group was injected with 500  $\mu\text{l}$  of FR-TPNP emulsion (50 mg/ml) via the tail vein; the non-targeted group was injected with 500  $\mu\text{l}$  of PNP emulsion (50 mg/ml); the lohexol group was injected with 500  $\mu\text{l}$  of lohexol (300 mg l/ml) via the tail vein; and the control group was injected with 500  $\mu\text{l}$  of pure PLGA nanoparticle emulsion (50 mg/ml). The in vivo CT scan parameters were as follows: tube voltage, 120 kV; tube current, 80 mA; section thickness, 0.625 mm; pitch, 0.562:1; and field of view (FOV), ped head. The CT images of the tumor, liver, and spleen in the four groups were acquired before and 5 min, 30 min, 2 h, 6 h, 12 h, 24 h and 48 h after injection. The mean CT

values within the ROIs of the tumor, liver and spleen were measured with a GE ADW 4.3 workstation.

#### Statistical analysis

Data are presented as the means  $\pm$  standard deviation (SD). Significant differences for multiple groups were determined using one-way ANOVA, and individual groups were compared using LSD. Probabilities of  $P < 0.05$  were considered significant.

## Results

### Characteristics of the FR-TPNPs

The FR-TPNPs with different PFOB: PLGA volume ratios were produced using a two-step emulsion technique. The emulsions were white milk-like in appearance. The FR-TPNPs were uniform and spherical, as observed by optical microscopy (**Figure 2A**). However, many oil-like droplets were visible using optical microscope imaging of the FR-TPNP emulsion (volume ratio of 1:1) (**Figure 2B**). The characteristics of the FR-TPNPs are provided in **Table 1**. SEM and TEM were used to observe the morphology directly. The FR-TPNPs had a spherical morphology, as shown in **Figure 3A**, and the structure was a shell-core structure with a dark domain in the center of the FR-TPNP (**Figure 3B**), which was not observed in the pure PLGA nanoparticles (**Figure 3C**).

### *In vitro CT-enhanced ability of FR-TPNPs*

The CT images indicated that the FR-TPNP emulsion (volume ratio of 1:8 to 1:2) was homogeneous and had a high density, whereas

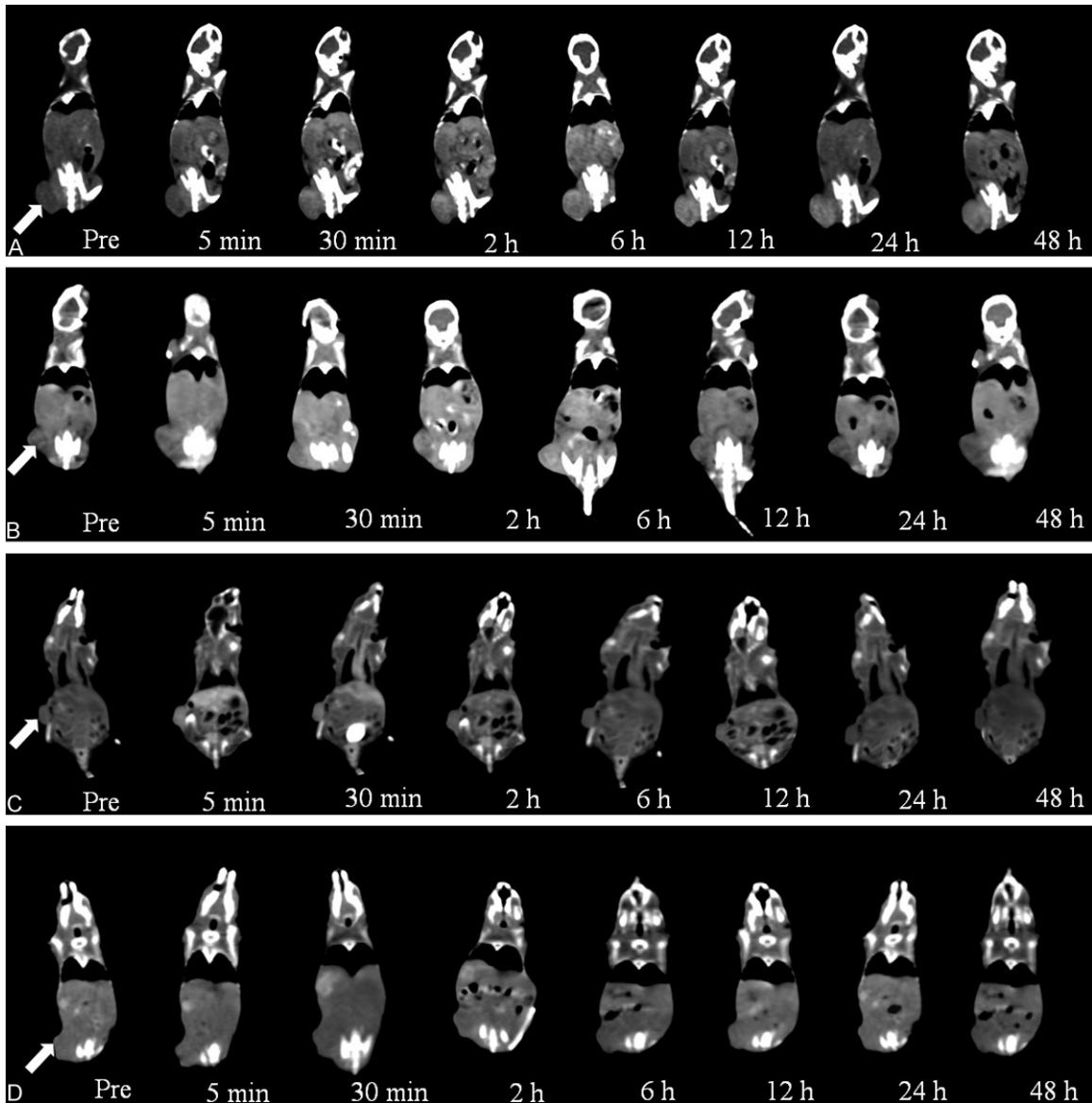


**Figure 6.** In vivo CT images of ovarian cancer xenografts at various times. A. Targeted group; B. Non-targeted group; C. Iohexol group; D. Control group. The arrows indicate the tumors.

the FR-TPNP emulsion (volume ratio of 1:1) was inhomogeneous with many high density features at the bottom, as shown in **Figure 4**. The mean CT value of the FR-TPNP (1:1) was significantly higher than those of the 1:4 and 1:8 groups ( $F = 31.428$ ,  $P < 0.05$ ), but there was no significant difference between the 1:1 and 1:2 groups ( $P > 0.05$ ).

#### *The in vitro targeting efficiency of FR-TPNPs*

A large number of red dots, representing FR-TPNPs, were observed in the cytoplasm of the SKOV3 cells, whereas few nanoparticles

remained within cancer cells in the control and folic acid intervention groups (**Figure 5**), demonstrating the greater cell affinity and targeting efficiency of FR-TPNPs than the PNPs to SKOV3 cells.

#### *In vivo tumor targeting ability of FR-TPNPs*

The in vivo targeted transportation of the FR-TPNPs was demonstrated by CT imaging (**Figure 6**) and the CT values (**Figure 7**). Five minutes after injection, the tumors were enhanced significantly in the Iohexol group, whereas no significant contrast enhancement

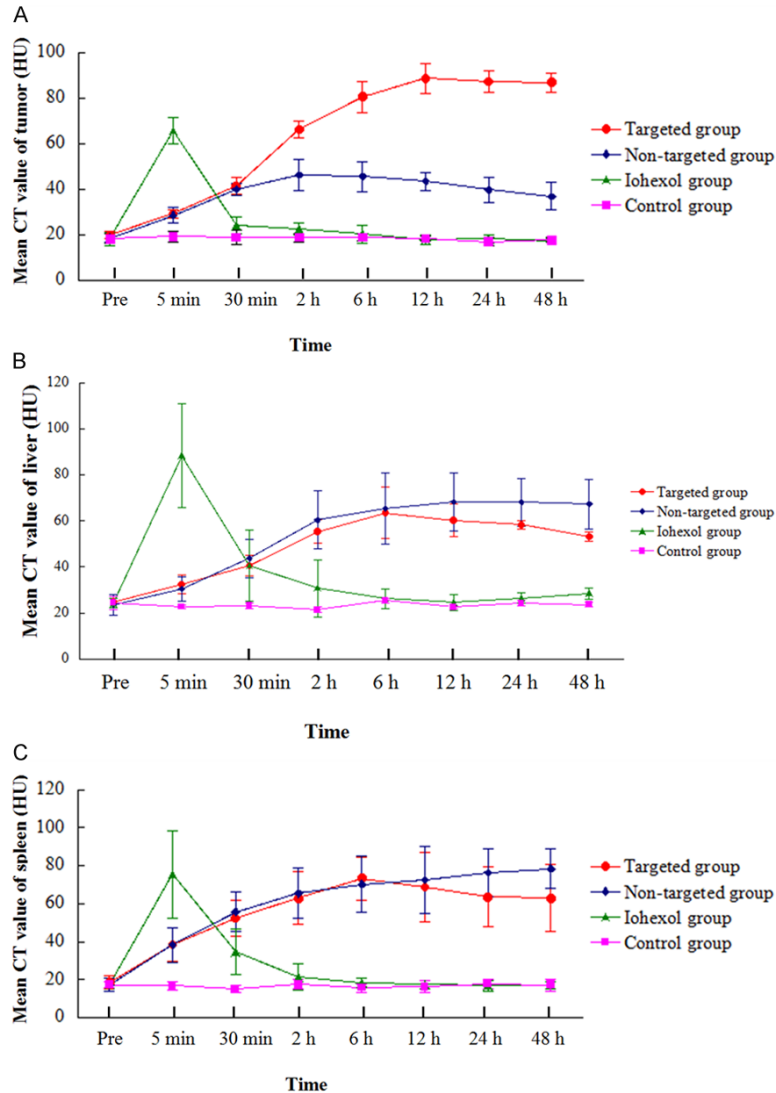


**Figure 7.** Histograms of the tumor, liver and spleen using different NPs. A. Tumor; B. Liver; C. Spleen.

of the tumors was observed in the targeted and non-targeted groups. The mean CT value of the tumors in the Iohexol group was considerably higher than those of the other groups ( $F = 90.292$ ,  $P < 0.05$ ). Thirty minutes after injection, the contrast enhancement of the tumor in the Iohexol group decreased rapidly, whereas the contrast enhancement of the targeted and non-targeted groups increased. The mean CT value of the tumor in Iohexol was lower than in the NP groups, but there were no differences in tumor contrast enhancement between the targeted and non-targeted groups within 30 min ( $F = 34.509$ ,  $P < 0.05$ ). The contrast enhancement of the tumors in the targeted group increased from 2 h to 12 h and had a

duration of up to 48 h after injection. The mean CT value of the tumors was significantly higher than those in the other groups from 2 to 48 h post-injection ( $F = 85.39$ ,  $95.318$ ,  $218.88$ ,  $221.68$ ,  $222.47$ ,  $P < 0.05$ ) and was also slightly higher than those of the liver and spleen in the targeted group 12 h post-injection ( $F = 36.231$ ,  $38.801$ ,  $20.932$ ,  $P < 0.05$ ).

There was no enhancement of the tumor, liver or spleen in the control group.

## Discussion

In this work, we used the PFOB as the X-ray attenuation core, which is a classic, highly biocompatible alternative for CT contrast-enhanced imaging. Because PFOB is hydrophobic and not miscible in oil, it must be emulsified for intravenous injection [20]. We synthesized the particles using a two-step emulsion technique. To optimize the synthetic conditions, we explored the effect of different PFOB: PLGA volume ratios on the emulsion synthesis. All volume ratios generated the emulsion,

but the size of the particles increased with the volume ratio. The size of the FR-TPNPs was maximized when the volume ratio was 1:1, and the PDI results indicated that the distribution was heterogeneous. This heterogeneity could result because the PFOB liquid and PLGA, which was dissolved in  $\text{CH}_2\text{Cl}_2$ , form a heterogeneous dispersion system when an external force is applied. The volume ratio of PLGA in the dispersion system decreases as the volume of PFOB is increased. Thus, the contact area is increased, and fusion of PFOB might occur in the emulsification process, indicating that more PFOB could be encapsulated in each particle, thus increasing the size of particle. Furthermore, according to Stokes' law, a smaller particle has

a slower sedimentation rate and thus results in a more stable emulsion. Thus, the prepared 1:1 emulsion of FR-TPNP was inhomogeneous, with larger particles located at the bottom; the other emulsions were more homogeneous and had smaller nanoparticles.

Nevertheless, the mean CT value of the emulsions increased with increasing volume ratios, and the mean CT value was highest for the 1:1 FR-TPNP emulsion. However, the mean CT value of this emulsion was not significantly higher than that of the 1:2 FR-TPNP emulsion. With respect to the nanoparticle size, PDI and CT-enhanced potential of the FR-TPNP emulsion, the 1:2 PFOB: PLGA volume ratio is most appropriate for synthesizing the emulsion for subsequent use in the *in vivo* experiment in this study.

The folate receptor is overexpressed on the surface of lung cancer, ovarian cancer and breast cells [21]. As a result, the folate receptor is thought to be an ideal target site for tumor molecular probes. Many researchers have prepared folate receptor targeting nanoparticles using the electrostatic adsorption technique, the streptavidin method and the carbodiimide method, among others [22, 23]. Despite the high targeting efficiency of these nanoparticles, their connection procedures are discontinuous and complex. In this study, we introduced Fol-PEG-COOH to the nanoparticles by dissolving it with PLGA, which is a simple and repeatable method for synthesizing the targeted shell of the nanoparticles. Furthermore, according to the results of the *in vitro* and *in vivo* targeted experiments, the FR-TPNPs prepared by this method have a high targeting efficiency for SKOV3 cells *in vitro* and were accumulated at higher levels in the ovarian cancer xenograft tumors than the PNPs, indicating the excellent targeting ability of FR-TPNPs.

Furthermore, the hydrophilic moiety of PEG on the particular surface of the nanoplatforms provides the steric hindrance necessary to shield against the reticuloendothelial system (RES), which is known as the “pegylation” method [24]. Thus, the introduction of Fol-PEG-COOH resulted in nanoparticles with a folate receptor targeting function and increased the steric stability for prolonged circulation in the blood. Therefore, PEGylated folate allows

FR-TPNP to avoid the RES, which allows a greater number of FR-TPNPs to accumulate in the tumor. This notion was confirmed in our *in vivo* experiment. The mean CT values of the liver and spleen tumors were considerably higher in the targeted groups.

However, there was a significant difference in the contrast-enhanced images of tumors between the targeted and non-targeted groups 2 h post-injection, especially after 6 h. This discrepancy could result because solid tumors typically have blood vessels with enhanced vascular permeability, which allows the extravasation of carrier materials with sizes of up to several hundreds of nanometers [25], and the sizes of the FR-TPNPs and PNPs were approximately 300 nm. Therefore, both of the NPs can leak through the vascular endothelia gap because of the enhanced permeability and retention (EPR) effect [26], eliminating the possibility of a significant difference between the two groups. The FR-TPNPs considered in this work were PEGylated nanoparticles. According to the *in vivo* kinetics of PFOB/PLGA nanocapsules reported by Odile et al. [27], the PEGylated PFOB/PLGA nanocapsule increases the residence time in the blood stream, which is not the case for plain nanocapsules; plain nanocapsules are deposited in the liver and spleen more rapidly than PEGylated nanocapsules. Thus, we hypothesize that a large number of FR-TPNPs might reside in the blood circulation for a longer time than PNPs. Furthermore, the FR-TPNPs can be continuously recognized by the tumor cells and accumulate in the tumor site at a later time, which was not the case for PNPs. This ability of the FR-TPNPs results in a significant increase in the CT value of tumors at later time points.

Moreover, in the *in vivo* experiment, we did not observe significant contrast enhancement of the kidney or bladder in the NP group, whereas Iohexol was eliminated rapidly in the kidneys. The difference in the excretion of the nanoparticles is due to their diameter. Nanoparticles with a diameter of less than 5 nm are thought to be swiftly excreted by the kidneys, whereas larger nanoparticles are not sufficiently small to pass through the kidneys and are thus retained in the bloodstream [28]. The rapid elimination of nanoparticles by the kidneys may result in serious adverse effects [29]. PLGA is known for

its biodegradability and biocompatibility; therefore, the FR-TPNPs may be safer than small-molecule iodinated agents for patients with renal insufficiency.

Persistent contrast enhancement of the tumor, liver and spleen in the NP groups was observed 48 h post-injection, which is later than in the Iohexol group only observed for 30 min). This difference indicates that the FR-TPNP emulsion is an effective contrast agent with a long circulation time and may be used for targeted therapy in the future.

There are several limitations to this study. First, the zeta potential of the FR-TPNPs was negative, which is unfavorable for interactions between the FR-TPNPs and negatively charged tumor cells. Second, the carrier rates of PFOB and Fol-PEG-COOH must be explored in the future. Because FR-TPNPs are capable of loading lipophilic drugs, we will conduct further studies to load chemotherapy drugs for targeted drug delivery in ovarian cancer.

### Conclusions

We have successfully developed a folate-receptor targeted CT contrast agent for ovarian cancer-targeted contrast-enhanced imaging. The applications of this targeted contrast agent may include detecting and diagnosing ovarian cancer and its metastases. Moreover, due to its long circulation time, this CT contrast agent could be multi-modal and eventually facilitate targeted drug delivery in ovarian cancer.

### Acknowledgements

The authors thank Mr. Weiguo Ni and Mr. Rui Pen for their assistance with CT imaging as well as Dr. Yajing Zhao for her help with the experiments. This work was supported by the National Nature Science of China (Grant No. 81130025).

### Disclosure of conflict of interest

None.

### Abbreviations

CLSM, confocal laser scanning microscope; CT, computed tomography; Fol-PEG-COOH, folate-poly (ethylene glycol)-carboxylic acid; FR-TPNP, folate-receptor targeting perfluorooctylbromide nanoparticle; PFOB, perfluorooctylbromide;

PLGA, poly (lactic-co-glycolic acid); PNP, perfluorooctylbromide nanoparticle; PVA, polyvinyl alcohol; SEM, scanning electron microscopy; TEM, transmission electron microscopy.

**Address correspondence to:** Jiannong Zhao, Department of Radiology, The Second Affiliated Hospital of Chongqing Medical University, No. 74 Linjiang Rd, Yuzhong District, Chongqing 400010, China. E-mail: ameng820311@163.com

### References

- [1] Jemal A, Siegel R, Ward E, Hao Y, Xu J, Murray T, Thun MJ. Cancer statistics. *CA Cancer J Clin* 2008; 58: 71-96.
- [2] Prat J. Ovarian carcinoma: five distinct diseases with different origins, genetic alterations, and clinicopathological features. *Virchows Arch* 2012; 460: 237-249.
- [3] Clarke-Pearson DL. Clinical practice. Screening for ovarian cancer. *N Engl J Med* 2009; 361: 170-177.
- [4] Bharali DJ, Khalil M, Gurbuz M, Simone TM, Mousa SA. Nanoparticles and cancer therapy: a concise review with emphasis on dendrimers. *Int J Nanomedicine* 2009; 4: 1-7.
- [5] Kalli KR, Oberg AL, Keeney GL, Christianson TJ, Low PS, Knutson KL, Hartmann LC. Folate receptor alpha as a tumor target in epithelial ovarian cancer. *Gynecol Oncol* 2008; 108: 619-626.
- [6] Van Dam GM, Themelis G, Crane LM, Harlaar NJ, Pleijhuis RG, Kelder W, Sarantopoulos A, de Jong JS, Arts HJ, van der Zee AG, Bart J, Low PS, Ntziachristos V. Intraoperative tumor-specific fluorescence imaging in ovarian cancer by folate recaptor-alpha targeting: first in-human results. *Nat Med* 2011; 17: 1335-1319.
- [7] Symanowski JT, Maurer AH, Naumann RW. Use of 99mTc-EC20 (a folate-targeted imaging agent) to predict response to therapy with EC145 (folate-targeting therapy) in advanced ovarian cancer [abstract]. *ASCO Meeting Abstracts* 2010; 28: 5034.
- [8] Liu TW, Stewart JM, Macdonald TD, Chen J, Clarke B, Shi J, Wilson BG, Zheng G. Biologically-targeted detection of primary and micro-metastatic ovarian cancer. *Theranostics* 2013; 3: 420-427.
- [9] Cai QY, Kim SH, Choi KS, Kim SY, Byun SJ, Kim KW, Park SH, Juhng SK, Yoon KH. Colloidal gold nanoparticles as a blood-pool contrast agent for x-ray computed tomography in mice. *Invest Radiol* 2007; 42: 797-806.
- [10] Xing H, Bu W, Ren Q, Zheng X, Li M, Zhang S, Qu H, Wang Z, Hua Y, Zhao K, Zhou L, Peng W, Shi J. A NaYbF<sub>4</sub>: Tm<sup>3+</sup> nanoprobe for CT and NIR-to-NIR fluorescent bimodal imaging. *Biomaterials* 2012; 33: 5384-5393.

## FR-TPNP as a targeted for early detection of ovarian cancer

- [11] Rabin O, Manuel Perez J, Grimm J, Wojtkiewicz G, Weissleder R. An X-ray computed tomography imaging agent based on longcirculating bismuth sulphide nanoparticles. *Nat Mater* 2006; 5: 118-122.
- [12] Pan D, Schirra CO, Wichline SA, Lanza GM. Multicolor computed tomographic molecular imaging with noncrystalline high-metal-density nanobecons. *Contrast Media Mol Imaging* 2014; 9: 13-25.
- [13] Mattrey RF. Perfluorooctylbromide-a new contrast agent for CT, sonography, and MR imaging. *Am J Roentgenol* 1989; 152: 247-252.
- [14] Mattrey RF, Long DM, Multer F, Mitten R, Higgins CB. Perfluorooctylbromide: a reticuloendothelial-specific and tumor-imaging agent for computed tomography. *Radiology* 1982; 145: 755-758.
- [15] Ao L, Yuanyi Z, Yu J, Wang Z, Yang Y, Wu W, Guo D, Ran H. Superparamagnetic perfluorooctylbromide nanoparticles as a multimodal contrast agent for US, MR, and CT imaging. *Acta Radiol* 2013; 54: 278-283.
- [16] Barnett BP, Ruiz-Cabello J, Hota P, Ouwerkerk R, Shablott MJ, Lauzon C, Walczak P, Glison WD, Chacko VP, Kraitchman DL, Arepally A, Bulte JW. Use of perfluorocarbon nanoparticles for non-invasive multimodal cell tracking of human pancreatic islets. *Contrast Media Mol Imaging* 2011; 6: 251-259.
- [17] Danhier F, Ansorena E, Silva JM, Coco R, Le Breton A, Preat V. PLGA-based nanoparticles: an overview of biomedical applications. *J Control Release* 2012; 161: 505-522.
- [18] Jin SE, Jin HE, Hong SS. Targeted delivery system of nanobiomaterials in anticancer therapy: from cells to clinics. *Biomed Res Int* 2014; 2014: 814208.
- [19] Duncan R. Polymer conjugates as anticancer nanomedicines. *Nat Rev Cancer* 2006; 6: 688-701.
- [20] Hill ML, Gorelikov I, Niroui F, Levitin RB, Mainprize JG, Yaffe MJ, Rowlands JA, Matsuura N. Towards a nanoscale mammographic contrast agent: development of a modular pre-clinical dual optical/x-ray agent. *Phys Med Biol* 2013; 58: 5215-5235.
- [21] Kalli KR, Oberg AL, Keeney GL, Christianson TJ, Low PS, Knutson KL, Hartmann LC. Folate receptor alpha as a tumor target in epithelial ovarian cancer. *Gynecol Oncol* 2008; 108: 619-626.
- [22] Kim DH, Klibanov AL, Needham D. The influence of tiered layers of surface-grafted poly(ethylene glycol) on receptor-ligand-mediated adhesion between phospholipid monolayer-stabilized microbubbles and coated glass beads. *Langmuir* 2000; 16: 2808-2817.
- [23] Weller GE, Wong MK, Modzelewski RA, Lu E, Klibanov AL, Wagner WR, Villanueva FS. Ultrasonic imaging of tumor angiogenesis using contrast microbubbles targeted via the tumor-binding peptide arginine-arginine-leucine. *Cancer Res* 2005; 65: 533-539.
- [24] Kommareddy S, Tiwari SB, Amiji MM. Longcirculating polymeric nanovectors for tumor-selective gene delivery. *Technol Cancer Res Treat* 2005; 4: 615-625.
- [25] Oeffinger BE, Wheatley MA. Development and characterization of a nano-scale contrast agent. *Ultrasonics* 2004; 42: 343-347.
- [26] Fang J, Nakamura H, Maeda H. The EPR effect: unique features of tumor blood vessels for drug delivery, factors involved, and limitations and augmentation of the effect. *Adv Drug Deliv Rev* 2011; 63: 136-151.
- [27] Diou O, Tsapis N, Giraudeau C, Valette J, Gueutin C, Bourasset F, Zanna S, Vauthier C, Fattal E. Long-circulating perfluorooctyl bromide nanocapsules for tumor imaging by 19FMRI. *Biomaterials* 2012; 33: 5593-5602.
- [28] Choi HS, Liu W, Liu F, Nasr K, Misra P, Bawendi MG, Frangioni JV. Renal clearance of quantum dots. *Nat Biotechnol* 2007; 25: 1165-1170.
- [29] Liu Y, Ai K, Lu L. Nanoparticulate X ray computed tomography contrast agents: from design validation to in vivo applications. *Acc Chem Res* 2012; 45: 1817-1827.